

### <sup>13</sup>C Line Narrowing by <sup>2</sup>H Decoupling in <sup>2</sup>H/<sup>13</sup>C/<sup>15</sup>N-Enriched Proteins. Application to Triple Resonance 4D *J* Connectivity of Sequential Amides

Stephan Grzesiek,<sup>†</sup> Jacob Anglister,<sup>†,‡</sup> Hao Ren,<sup>§</sup> and Ad Bax<sup>\*,†</sup>

Laboratory of Chemical Physics, National Institute of Diabetes and Digestive and Kidney Diseases, and Laboratory of Biochemistry, National Cancer Institute  
National Institutes of Health, Bethesda, Maryland 20892

Received February 3, 1993

Short transverse <sup>13</sup>C relaxation times, *T*<sub>2</sub>, constitute the principal barrier for the application of heteronuclear *J* correlation NMR techniques to larger proteins uniformly enriched with <sup>13</sup>C and <sup>15</sup>N.<sup>1–6</sup> The <sup>13</sup>C *T*<sub>2</sub> is dominated by the strong dipolar interaction with its attached protons.<sup>7</sup> As the magnetogyric ratio of <sup>2</sup>H is ~6.5 times lower than that of <sup>1</sup>H, the heteronuclear dipolar interaction is greatly reduced by deuteration. Because of the large <sup>2</sup>H quadrupolar interaction (~170 kHz), the <sup>2</sup>H spin lattice relaxation time, *T*<sub>1</sub>, in proteins is in the millisecond range at a magnetic field strength of 14 T. Therefore, the <sup>2</sup>H–<sup>13</sup>C *J* coupling (~22 Hz) does not result in the triplet shape, expected for a <sup>13</sup>C nucleus coupled to a spin-1 nucleus, but gives rise to a collapsed singlet resonance that is broadened by scalar relaxation of the second kind.<sup>8,9</sup> High-power (~2.5 W) <sup>2</sup>H decoupling with an RF field strength much stronger than the inverse <sup>2</sup>H *T*<sub>1</sub> effectively removes this broadening and results in a <sup>13</sup>C line width that is much narrower than for the protonated <sup>13</sup>C.

One of the triple resonance *J* correlation experiments affected most by the <sup>13</sup>C line width is the H(CA)NH experiment<sup>10,11</sup> which relies on magnetization transfer from C<sup>α</sup> to the backbone <sup>15</sup>N nucleus via the relatively small <sup>1</sup>*J*<sub>NC<sup>α</sup></sub> (~11 Hz) and <sup>2</sup>*J*<sub>NC<sup>α</sup></sub> (~5–8 Hz)<sup>12</sup> couplings. Although experiments have been proposed to alleviate this difficult *J* correlation step,<sup>13,14</sup> the sequential assignment procedure which is based on *J* correlation between the intrasidue <sup>1</sup>H/<sup>15</sup>N and <sup>1</sup>H/<sup>13</sup>C<sup>α</sup> resonances and between the <sup>1</sup>H/<sup>13</sup>C<sup>α</sup> of residue *i* and <sup>1</sup>H/<sup>15</sup>N of residue *i* + 1 is complicated by the high degree of overlap among <sup>1</sup>H/<sup>13</sup>C<sup>α</sup> correlations. Here we describe a procedure which allows *J* correlation between the much better resolved <sup>1</sup>H/<sup>15</sup>N resonances of sequential residues, thereby bypassing the overlapping <sup>1</sup>H/<sup>13</sup>C<sup>α</sup> pairs. Efficient transfer of magnetization from <sup>13</sup>C<sup>α</sup> to <sup>15</sup>N is possible in the present case because of the <sup>13</sup>C<sup>α</sup> line narrowing afforded by deuteration and <sup>2</sup>H decoupling.

Briefly the scheme of Figure 1 functions as follows. After H<sup>N</sup><sub>*i*+1</sub> evolution during *t*<sub>1</sub>, magnetization is transferred to its attached nucleus N<sub>*i*+1</sub> (time *a*). Following a constant time evolution period, *t*<sub>2</sub>, during which <sup>13</sup>C<sup>α</sup> is decoupled from <sup>15</sup>N, the <sup>15</sup>N<sub>*i*+1</sub> magnetization is relayed via <sup>13</sup>CO<sub>*i*</sub> (time *b*) and <sup>13</sup>C<sup>α</sup><sub>*i*</sub> magnetization (time *c*) to the <sup>15</sup>N<sub>*i*</sub> of residue *i* (time *d*). The effect of dephasing caused by the homonuclear <sup>13</sup>C<sup>α</sup>–<sup>13</sup>C<sup>β</sup> *J* coupling during the period where C<sup>α</sup> magnetization is transferred ( $\eta = \eta_1 + \eta_2 + \eta_3$ ) is effectively eliminated by setting  $\eta$  to  $\sim 1/J_{CC}$  (27.6 ms). At time *d*, a fraction  $\sin[\pi\eta(^1J_{NC\alpha})] \cos[\pi\eta(^2J_{NC\alpha})]$  of the C<sup>α</sup> magnetization is transferred to the intrasidue <sup>15</sup>N, and a smaller fraction,  $\sin[\pi\eta(^2J_{NC\alpha})] \cos[\pi\eta(^1J_{NC\alpha})]$ , is transferred back to the amide from which magnetization originated. After the second <sup>15</sup>N constant time evolution period, *t*<sub>3</sub>, (time *e*), magnetization is transferred by means of a reverse INEPT sequence to H<sup>N</sup> for observation. In the 4D spectrum, the frequency coordinates of *J* correlations in the *F*<sub>1</sub>, *F*<sub>2</sub>, *F*<sub>3</sub>, and *F*<sub>4</sub> dimensions then correspond to the chemical shifts of H<sup>N</sup><sub>*i*+1</sub>, N<sub>*i*+1</sub>, N<sub>*i*</sub>, and H<sup>N</sup><sub>*i*</sub>, respectively. The “diagonal peaks” at H<sup>N</sup><sub>*i*+1</sub>, N<sub>*i*+1</sub>, H<sup>N</sup><sub>*i*+1</sub>, and N<sub>*i*+1</sub>, due to the above mentioned two-bond *J*<sub>NC<sup>α</sup></sub> transfer process, are 2–4 times weaker.

Experiments are conducted on a Bruker AMX-600 spectrometer, modified such that the <sup>2</sup>H lock receiver is disabled during <sup>2</sup>H decoupling. Details regarding this hardware modification will be published elsewhere. The method is demonstrated for a sample containing ~1.4 mM of the protein calcineurin B (19.7 kD), uniformly enriched with <sup>2</sup>H, <sup>15</sup>N, and <sup>13</sup>C to levels of 50%, 98%, and 88%, respectively. A second sample, with higher deuteration (~85%), was also prepared to illustrate directly the <sup>13</sup>C line narrowing obtainable. The fact that the deuteration level of the sample used for the 4D experiment is only 50% lowers the sensitivity of this particular experiment, but it permits this sample to be used also for a large range of other experiments that require partial side-chain protonation. Both samples also contain 20 mM CaCl<sub>2</sub> and 20 mM CHAPS, a zwitterionic detergent which was shown not to significantly affect the structure or binding affinity of calcineurin B.<sup>15</sup> Experiments were conducted at 37 °C, pH 5.6.

Figure 2 illustrates the <sup>13</sup>C resolution enhancement obtained by deuteration and <sup>2</sup>H decoupling for a small region of the 2D H(N)CA correlation spectrum,<sup>16</sup> displaying connectivities between amide protons and their intrasidue C<sup>α</sup>. In the absence of deuteration and <sup>2</sup>H decoupling, the <sup>13</sup>C<sup>α</sup> resonance is a poorly resolved doublet, split by <sup>1</sup>*J*<sub>CC</sub> coupling with <sup>13</sup>C<sup>β</sup>, with a line width for the doublet components of ca. 25 Hz (Figure 2A). In the case of deuteration and <sup>2</sup>H decoupling, the C<sup>α</sup> doublet is well-resolved with line widths of ~10 Hz (Figure 2B). The <sup>13</sup>C<sup>α</sup> resonances in the deuterated protein are shifted upfield by ~0.35 ppm, caused primarily by the one-bond <sup>2</sup>H isotope effect. The 10-Hz <sup>13</sup>C<sup>α</sup> line width is determined primarily by the limited acquisition time in the *t*<sub>1</sub> dimension of the 2D H(N)CA experiment, and by incomplete deuteration of the amino acid side chains which results in a distribution of two- and three-bond isotope effects.

Figure 3 shows four cross sections through the 4D HN(COCA)-NH spectrum, illustrating *J* connectivities between the amides of residues F72–F75. Of all the sequential *J* connectivities expected on the basis of the backbone assignments,<sup>17</sup> 98% were observed, except for a stretch of residues close to the C154K mutation, which causes line broadening of the resonances.<sup>17</sup>

Previous attempts to demonstrate the <sup>13</sup>C line narrowing

<sup>†</sup> National Institute of Diabetes and Digestive and Kidney Diseases.

<sup>‡</sup> On leave from The Weizmann Institute, Rehovot, Israel.

<sup>§</sup> National Cancer Institute.

(1) Oh, B. H.; Westler, W. M.; Derba, P.; Markley, J. L. *Science* **1988**, *240*, 908–911.

(2) Ikura, M.; Kay, L. E.; Bax, A. *Biochemistry* **1990**, *29*, 4659–4667.

(3) Boucher, W.; Laue, E. D.; Campbell-Burk, S.; Domaille, P. J. *J. Am. Chem. Soc.* **1992**, *114*, 2262–2264.

(4) Olejniczak, E. T.; Xu, R. X.; Fesik, S. W. *J. Biomol. NMR* **1992**, *2*, 655–659.

(5) Palmer, A. G., III; Fairbrother, W. J.; Cavanagh, J.; Wright, P. E.; Rance, M. J. *Biomol. NMR* **1992**, *2*, 103–108.

(6) Grzesiek, S.; Döbeli, H.; Gentz, R.; Garotta, G.; Labhardt, A. M.; Bax, A. *Biochemistry* **1992**, *31*, 8180–8190.

(7) Browne, D. T.; Kenyon, G. L.; Packer, E. L.; Sternlicht, H.; Wilson, D. M. *J. Am. Chem. Soc.* **1973**, *95*, 1316–1323.

(8) Abragam, A. *The Principles of Nuclear Magnetism*; Clarendon Press: Oxford, 1961; p 309.

(9) London, R. E. *J. Magn. Reson.* **1990**, *86*, 410–415.

(10) Montelione, G. T.; Wagner, G. *J. Magn. Reson.* **1990**, *87*, 183–188.

(11) Kay, L. E.; Ikura, M.; Bax, A. *J. Magn. Reson.* **1991**, *91*, 84–92.

(12) Delaglio, F.; Torchia, D. A.; Bax, A. *J. Biomol. NMR* **1991**, *1*, 439–446.

(13) Clubb, R. T.; Thanabal, V.; Wagner, G. *J. Biomol. NMR* **1992**, *2*, 203–210.

(14) Clubb, R. T.; Thanabal, V.; Wagner, G. *J. Magn. Reson.* **1992**, *97*, 213–217.

(15) Anglister, J.; Grzesiek, S.; Ren, H.; Klee, C. B.; Bax, A. *J. Biomol. NMR* **1993**, *3*, 121–126.

(16) Grzesiek, S.; Bax, A. *J. Magn. Reson.* **1992**, *96*, 432–440.

(17) Anglister, J.; Grzesiek, S.; Ren, H.; Klee, C. B.; Bax, A. Unpublished results.

(18) LeMaster, D. M.; Richards, F. M. *Biochemistry* **1988**, *27*, 142–150.

(19) Shaka, A. J.; Lee, C. J.; Pines, A. *J. Magn. Reson.* **1988**, *77*, 274–293.

(20) Bax, A.; Pochapsky, S. S. *J. Magn. Reson.* **1992**, *99*, 638–643.

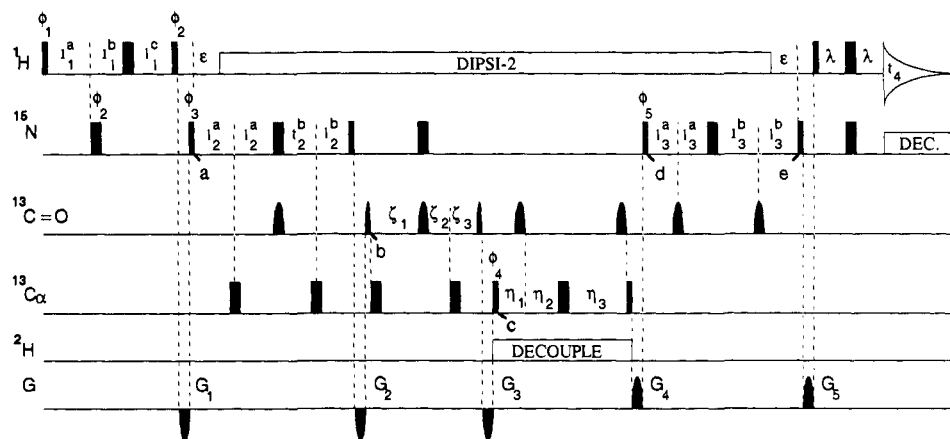


**Figure 1.** Pulse scheme of the HN(COCA)NH experiment. Narrow pulses correspond to a flip angle of  $90^\circ$ , wide pulses to  $180^\circ$ . Pulses for which the RF phase is not marked are applied along the  $x$  axis. Carbonyl pulses have a  $\sin x/x$ -center-lobe amplitude profile. Carrier frequencies are set to 4.66, 116.5, 177, 56, and 4 ppm for the  $^1\text{H}$ ,  $^{15}\text{N}$ ,  $^{13}\text{C}=\text{O}$ ,  $^{13}\text{C}\alpha$ , and  $^2\text{H}$  nuclei, respectively.  $^1\text{H}$  and  $^{15}\text{N}$  pulses are applied at 25 and 6 kHz, whereas the  $^{13}\text{C}\alpha$  ( $^{13}\text{C}=\text{O}$ )  $90^\circ$  and  $180^\circ$  pulses have durations of 53 and 47.4  $\mu\text{s}$  (219 and 300  $\mu\text{s}$ ), respectively. The  $^1\text{H}$  decoupling (DIPSI-2)<sup>19</sup>,  $^{15}\text{N}$  (WALTZ-16), and  $^2\text{H}$  (cw) decoupling are applied at field strengths of 5, 1.5, and 1.6 kHz, respectively. Phase cycling is as follows:  $\phi_1 = x$ ;  $\phi_2 = y, -y$ ;  $\phi_3 = x$ ;  $\phi_4 = 2(x), 2(-x)$ ;  $\phi_5 = x$ ;  $\text{acq} = x, 2(-x), x$ . Pulsed field gradients are used to suppress artifacts, not to select a coherence transfer pathway.<sup>20</sup> Gradients have a sine bell amplitude profile with a strength of 10 G/cm at their center. Durations are  $G_{1,2,3,4,5} = 0.85, 0.25, 0.35, 1.50, 4.00$  ms. Quadrature in the  $t_1, t_2$ , and  $t_3$  domains is obtained by changing the phases  $\phi_1, \phi_3$ , and  $\phi_5$ , respectively, in the usual states-TPP1 manner.<sup>21</sup> Delay durations are as follows:  $\epsilon = 5.4$  ms;  $\lambda = 2.25$  ms;  $\zeta_{1,2,3} = 11.1, 6.5, 4.6$  ms;  $\eta_{1,2,3} = 4.8, 9.0, 13.8$  ms. The initial delays for the semi-constant-time<sup>22</sup> evolution period ( $t_1$ ) and constant time evolution periods ( $t_2$  and  $t_3$ ) are set to  $t_{1,2,3}^{\text{a,b,c}} = 2.25, 0, 2.25$  ms;  $t_{2,3}^{\text{a,b}} = 5.6$  ms;  $t_{3,4,5}^{\text{a,b}} = 6.8$  ms. Increments for those delays are set to  $\Delta t_{1,2,3}^{\text{a,b,c}} = 354, 204, -102$   $\mu\text{s}$ ;  $\Delta t_{2,3}^{\text{a,b}} = 275, -275$   $\mu\text{s}$ ;  $\Delta t_{3,4,5}^{\text{a,b}} = 275, -275$   $\mu\text{s}$ .

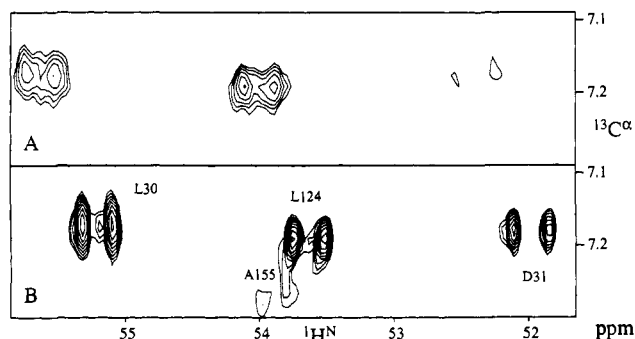


**Figure 2.** Small regions of the 2D H(N)CA spectrum of (A) fully protonated calcineurin B and (B) randomly 85%-deuterated calcineurin B, with  $^2\text{H}$  decoupling. Both spectra were recorded and processed identically. The  $t_1$  and  $t_2$  acquisition times used are 73 and 55 ms, respectively, and data are zero filled to yield a digital resolution of 5 Hz ( $F_1$ ) and 9 Hz ( $F_2$ ), with no digital filtering in the  $t_1$  dimension.

obtained by deuteration and  $^2\text{H}$  decoupling were only partially successful because the rapid  $^2\text{H}$  spin lattice relaxation at the low magnetic field strength used (1.4 T) required a stronger  $^2\text{H}$  decoupling field than could be generated experimentally.<sup>7</sup> At the high magnetic field strength used in our present work (14 T),  $^2\text{H}$   $T_1$  relaxation is much longer, and in addition, the  $^2\text{H}$  decoupling field used in our study is nearly 7 times stronger.

Random fractional deuteration, previously explored in homonuclear  $^1\text{H}$  NMR,<sup>18</sup> presents a powerful approach for overcoming the natural line width problem in heteronuclear NMR studies of larger  $^{13}\text{C}/^{15}\text{N}$ -enriched proteins. The present experiment is only a single example of the utility of this approach, but a large range of experiments that can benefit from deuteration is presently under investigation.

**Acknowledgment.** We thank Claude Klee for enthusiastic support of the calcineurin B NMR study, Geerten Vuister and

(21) Marion, D.; Ikura, M.; Tschudin, R.; Bax, A. *J. Magn. Reson.* **1989**, *85*, 393-399.

(22) Grzesiek, S.; Bax, A. *J. Biomol. NMR* **1993**, *3*, 185-204.

(23) Zhu, G.; Bax, A. *J. Magn. Reson.* **1990**, *90*, 405-410.

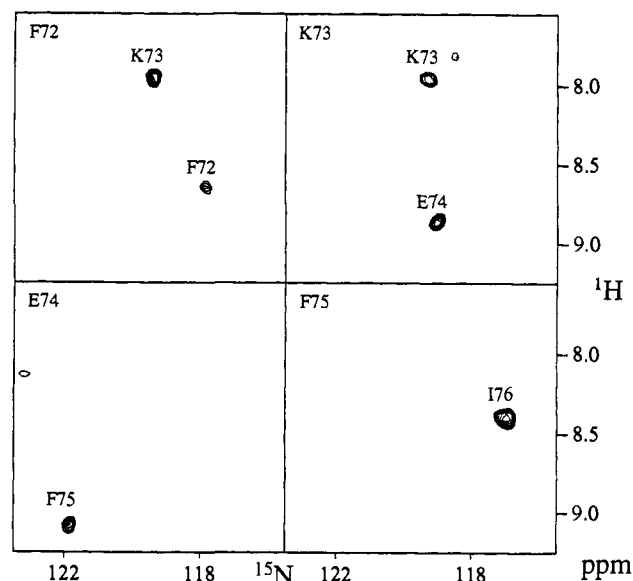


**Figure 3.** Four ( $F_1, F_2$ ) cross sections through the 4D HN(COCA)NH spectrum of calcineurin B (50%  $^2\text{H}$ ), taken at the ( $F_3, F_4$ ) frequencies of the amides of residues F72-F75. Each cross section shows the connection to amide  $^{15}\text{N}$  and  $^1\text{H}$  frequencies of the next residue; panels for F72 and K73 also show the weaker (4D) diagonal peaks to the same residue. The 4D spectrum results from a  $22^* \times 20^* \times 24^* \times 512^*$  data matrix, where  $n^*$  refers to  $n$  complex data points. Total accumulation time was 6 days with 32 scans per hypercomplex  $t_1, t_2, t_3$ -increment. Acquisition times were 14.5 ms ( $t_1$ ), 22.0 ms ( $t_2$ ), 26.4 ms ( $t_3$ ), and 55.3 ms ( $t_4$ ). The  $t_2$  and  $t_3$  time domains were extended by means of mirror image linear prediction<sup>23</sup> prior to zero filling and Fourier transformation. The size of the absorptive part of the final 4D spectrum was  $64 \times 128 \times 128 \times 1024$ .

Andy Wang for useful comments, and Rolf Tschudin for spectrometer hardware modification. This work was supported by the Intramural AIDS Targeted Anti-Viral Program of the Office of the Director of the National Institutes of Health.